

Flexible Edge Detection of Cuboidal Containers with a Wire Frame Model for Robot Based Plastic Welding

Philipp Gawron¹, Stefan Klug¹, Nikolai Hangst¹, Thomas M. Wendt¹ and Stefan J. Rupitsch²

¹ Work-Life Robotics Institute, Offenburg University of Applied Sciences, 77652 Offenburg, Germany

² Laboratory for Electrical Instrumentation and Embedded Systems, Department of Microsystems Engineering, University of Freiburg, 79110 Freiburg, Germany
philipp.gawron@hs-offenburg.de

Summary: Plastic welding is essential to fabricate process tanks in the field of semiconductor industries. Applying robot-assisted welding processes requires defining welding paths. Utilizing CAD/CAM or teach-in is both time-consuming. In this contribution, we describe and discuss two approaches to automatically measure and extract welding paths with the robot. These approaches enable a flexible detection of welding-paths for automated plastic welding of cuboid containers.

Keywords: Plastic welding, robot, tactile, laser triangulation, edge detection

Introduction

Plastic containers are utilized as process tanks in the field of special machine construction for the semiconductor industry. These containers may vary in size but are usually of cuboid form. The materials for the containers or tubing require to be resistant to various chemicals like strong acids, bases or cleaning solutions like Piranha, SC1 or SC2 [1]. Consequently, materials like poly vinylidene fluoride (PVDF), perfluoroalkoxy (PFA) or poly tetrafluoroethylene (PTFE) are used [1]. These materials are usually welded manually to join the container parts. Hot gas welding [2] and extrusion welding [3] processes are mainly applied for joining. Handling such welding equipment over the course of a working day is physically demanding. Fewer workers are available due to the shortage of skilled labor. Hence, robot-assisted plastic welding should be utilized to reduce the strain on humans. For metal welding robots with vision sensors like laser scanners are deployed, capable of seam tracking and finding [4]. These applied sensors require a separate workstation or control unit for data evaluation [4]. In [5] a robotic system for friction stir welding of polymers is presented and a force/torque sensor is applied to ensure contact between tool and welding surface. Automated welding path detection in the containers by the robot itself would shorten programming.

There are currently two ways to program the welding paths on the robot. The CAD/CAM system requires an absolutely measured cell, offline programming, a CAD-model and checking the program before execution. Another approach is the teach-in method, which applies manual setting of path points by the operator to program the robot. Setting the points is time-consuming and error-prone, especially in poorly visible areas such as the container's corners. The welding shoes for plastic require surface contact dur-

ing the welding process. Therefore, seam finding is crucial for the seam's quality. For fillet welds [6] by extrusion welding, a so-called floating skin may show up due to poor surface contact between the welding shoe and the two container walls. In this contribution, we investigate how welding paths can be determined automatically on the welding object by the robot.

Methods and Materials

Two seam finding approaches for fillet welds were investigated. First, a collaborative robot's integrated torque sensors were utilized in a tactile approach. Second, a single laser triangulation sensor was applied to detect specific points and calculate the container's dimensions.

Robot Assisted Plastic Welding

An extruder for plastic welding was adapted to a YASKAWA HC20 DTP, see Fig. 1. The robot has internal torque sensors for the detection of a collision with an object. Containers are welded from the inside with fillet welds to prevent leakage. Fig. 2 shows fillet welding with an extruder and the produced seam on a test specimen. Fig. 3 (left) depicts the specimen's cross section consisting of two parts and the fillet welding seam in orange. Fig. 3 (right) shows the extruder's welding shoe with surface contact on both parts.

Tactile Approach

In this approach, the robot performs a movement in X-direction first, see Fig. 4 (left) orange arrow to T1. The robot will stop when detecting the specimen, see Fig. 4 (right). For this purpose, the torque sensors of the utilized collaborative robot are read out until a certain threshold value for the torque is exceeded. The robot is then stopped and the current TCP-position is stored, achieving position T1. This gets repeated for the

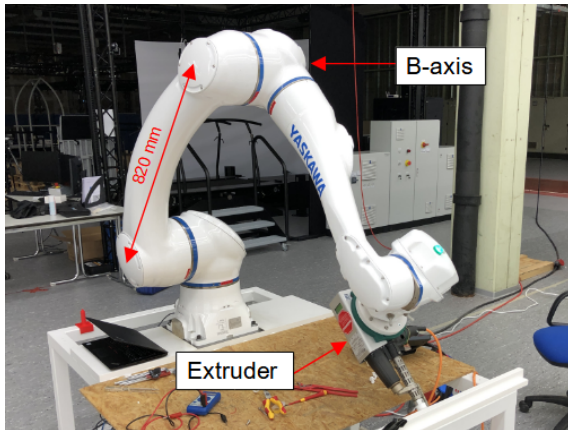


Fig. 1: Extruder welding with robot.

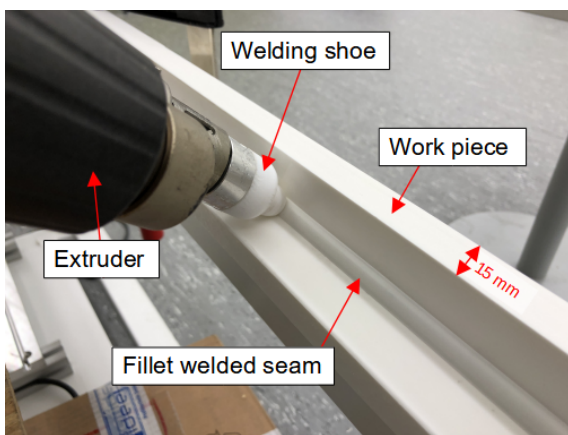


Fig. 2: Extruder welding with robot and fillet welded seam.

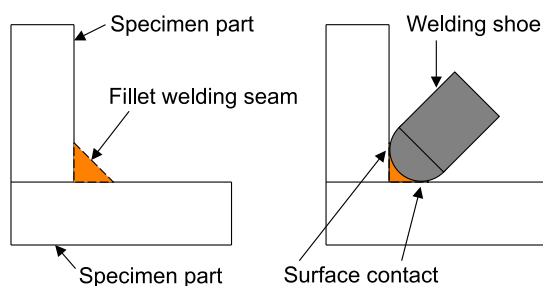


Fig. 3: Fillet welding, (left) cross section of a fillet welding seam, (right) welding shoe with surface contact.

Z-direction achieving T2. Combining T1 with the Z-value of T2 yields T3. This marks the position of the corner. Repeating this process on another point along the fillet leads to T4, T5 and finally T6. This allows performing a linear movement from T3 to T6.

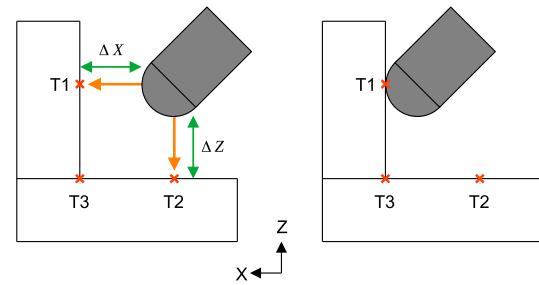


Fig. 4: Tactile measurement process, (left) required points T1 and T2 to calculate the specimen's corner T3, (right) detection of T1.

Laser Triangulation Approach

The container's orientation was assumed leveled with the robot's base. Therefore, rotation around the X or Y axis are not considered in this approach.

Measuring points and creating vectors

First, various points on each plane of the container are measured, see Fig. 5 (left). A vector is then created with two of these points. This is repeated for each vector shown in Fig. 5 (right).

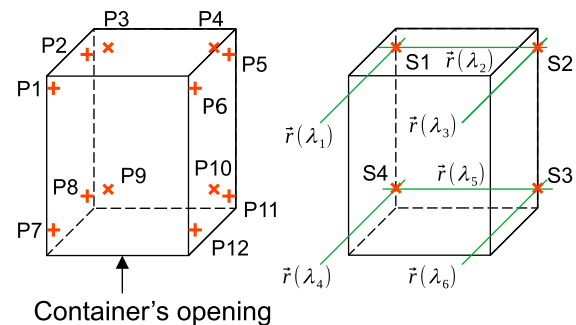


Fig. 5: Laser triangulation approach, (left) measured points inside the container on the left, right and rear shell, (right) calculated vectors and intersections.

Calculating intersections

Then, the intersections positions are calculated to yield the points S1...S4, see Fig. 5 (right). For example, S1 can be calculated with the two vectors [7]

$$\vec{r}(\lambda_1) = \vec{r}_1 + \lambda_1 \vec{a}_1 \quad (1)$$

$$\vec{r}(\lambda_2) = \vec{r}_2 + \lambda_2 \vec{a}_2 \quad (2)$$

with $(\lambda_1, \lambda_2) \in \mathbb{R}$. Equating $\vec{r}(\lambda_1)$ and $\vec{r}(\lambda_2)$ yields

$$\vec{r}_1 + \lambda_1 \vec{a}_1 = \vec{r}_2 + \lambda_2 \vec{a}_2. \quad (3)$$

Solving this system of linear equations provides λ_1^* and λ_2^* . The position vector for the intersection S1 is calculated

by inserting λ_1^* and λ_2^* in (1) or (2) [7]. This procedure gets repeated for S2...S4.

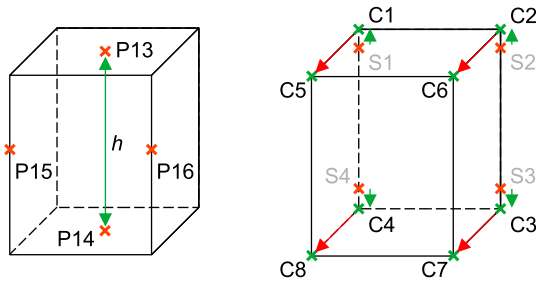


Fig. 6: Laser triangulation approach, (left) measured points on upper/lower shell and on the container's edges, (right) shifting the intersections to the container's corners.

Height-correction

Points on the upper (P13) and lower shell (P14) as well as the container's edges (P15, P16) are measured, see Fig. 6 (left). The container's height h is given by the points P15 and P16. The Z-value for S1...S4 is corrected resulting in the corners positions C1...C4, see the green arrows in Fig. 6 (right).

Calculating remaining points and generating welding paths

Utilizing the points P15 and P16 from the container's edges allows shifting C1...C4 yielding C5...C8. Once the points C1...C8 are known, these are applied to create welding paths for the fillet welding seams.

Results and Discussion

Tactile Approach

The tactile approach was evaluated with the robot HC20 and T-joint specimen. In order to achieve a precise stop of the robot to prevent damaging the extruder, we conducted the measurement in increments of 0.1 mm. The robot's B-axis was used for the torque-measurement. Due to the lever arm it showed the highest sensitivity compared to the other axes in the utilized pose. Fig. 7 shows the measurement in X-direction when the robot stopped. A benefit of this approach is the compensation of the differing welding shoe dimensions (e. g., manufacturing tolerances or abrasion) since absolute positions of the tool are measured. The internal torque sensors can also be applied to ensure a constant force between welding shoe and specimen during the welding process. A drawback is the slow search-movement resulting in a long measuring time. For example, the duration of the tactile measuring sequence for one corner (X and

Z) took 41 s, depending on the initial distance between welding shoe and specimen. Additionally, the robot's and the extruder's geometries may interfere with the container's walls during the measurement and reorientation.

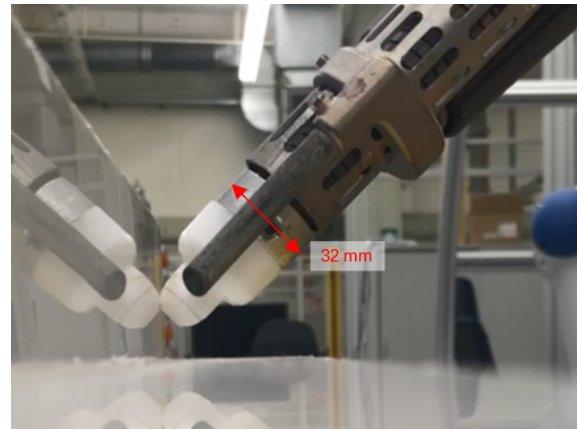


Fig. 7: Tactile measurement in X-direction.

Laser Triangulation Approach

This approach was evaluated with a KUKA KR600 with a single laser triangulation sensor and a pen mounted on the robot's flange, see Fig. 8. The sensor was applied for the measurements and the pen as evaluation. For evaluation, a test specimen for a single corner, see Fig. 9, as well as a cardboard box were utilized [8], see Fig. 10. Once the robot measured the required points to generate the vectors, the pen's tip was moved into the calculated corner, see Fig. 9, Fig. 12 and Fig. 11. Because of the single sensor utilized, the robot had to change the sensors orientation for each shell of the container. In comparison to the tactile measurement for one corner (X and Z of T-joint specimen), the lasers triangulation approach took around 12 s.

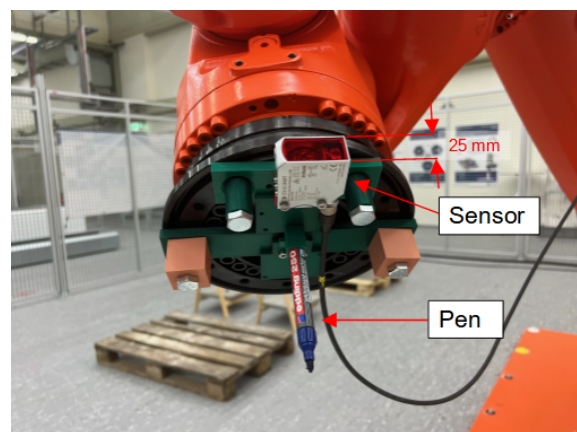


Fig. 8: Sensor and pen mounted on robot flange.

Conclusion

Both approaches showed good results regarding the corner-detection. The triangulation-approach has the benefit of being contactless, enabling faster measurements and, therefore, an overall better efficiency. Additionally, our approach does not require a separate control unit for data evaluation compared to laser profile sensors. The calculations can be carried out on the robot's control unit. The tactile approach has longer measurement cycles but compensates welding shoe tolerances. This work provides a contribution to the automation of plastic welding. Future work will focus on enhancing the triangulation-approach.

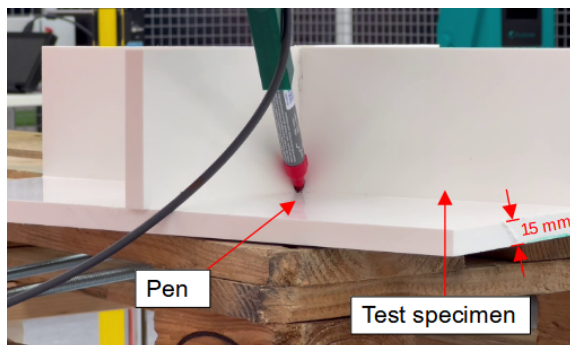


Fig. 9: Test specimen for corner detection.



Fig. 10: Cardboard box measurement.

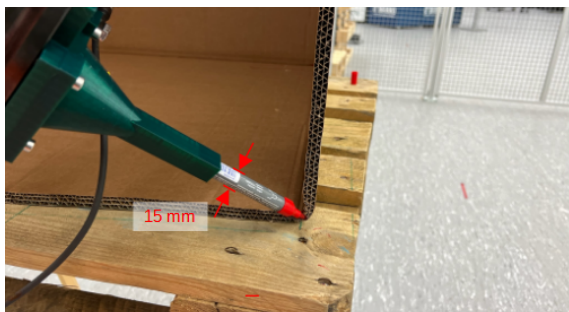


Fig. 11: Evaluation of measurement with a pen in the front corner.

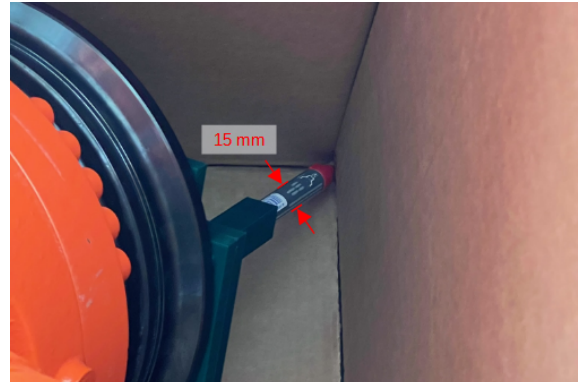


Fig. 12: Evaluation of measurement with a pen in the rear corner.

References

- [1] C. W. Extrand, "The use of fluoropolymers to protect semiconductor materials," *Journal of Fluorine Chemistry*, vol. 122, no. 1, pp. 121–124, 2003.
- [2] O. Balkan, H. Demirer, A. Ezdeşir, and H. Yıldırım, "Effects of welding procedures on mechanical and morphological properties of hot gas butt welded pe, pp, and pvc sheets," *Polymer Engineering & Science*, vol. 48, no. 4, pp. 732–746, 2008.
- [3] S. T. Amancio-Filho and J. F. dos Santos, "Joining of polymers and polymer–metal hybrid structures: Recent developments and trends," *Polymer Engineering & Science*, vol. 49, no. 8, pp. 1461–1476, 2009.
- [4] R. P. Manorathna, P. Phairatt, P. Ogun, T. Widjanarko, M. Chamberlain, L. Justham, S. Marimuthu, and M. R. Jackson, "Feature extraction and tracking of a weld joint for adaptive robotic welding," in *2014 13th International Conference on Control Automation Robotics & Vision (ICARCV)*, pp. 1368–1372, IEEE, 2014.
- [5] N. Mendes, P. Neto, M. A. Simão, A. Loureiro, and J. N. Pires, "A novel friction stir welding robotic platform: welding polymeric materials," *The International Journal of Advanced Manufacturing Technology*, vol. 85, no. 1-4, pp. 37–46, 2016.
- [6] J. Rotheiser, *Joining of plastics: Handbook for designers and engineers*. Cincinnati, Ohio and Munich: Hanser, 3. ed. ed., 2009.
- [7] L. Papula, *Mathematik für Ingenieure und Naturwissenschaftler: Ein Lehr- und Arbeitsbuch für das Grundstudium*. Viewegs Fachbücher der Technik, Wiesbaden: Vieweg+Teubner Verlag, 10., erweiterte auflage ed., 2001.
- [8] S. Klug, *Entwicklung eines sensorbasierten Kunststoffschweißprozesses mittels Industrieroboter*. Masterthesis, Hochschule Offenburg, 27. Oktober 2023.